

# Internal state distribution of alkali dimers in supersonic nozzle beams\*

M. P. Sinha, A. Schultz<sup>†</sup>, and R. N. Zare

*Department of Chemistry, Columbia University, New York, New York, 10027*

(Received 9 May 1972)

By spectroscopically analyzing the white light and laser-induced fluorescence excited in a nozzle beam of  $\text{Na}_2$  molecules, we have measured the population distribution of the  $(v, J)$  levels of the ground state. The  $\text{Na}_2$  molecules are produced in nozzle beams with various stagnation pressures (50–240 torr) of alkali metal and with nozzles of different throat diameters (0.12–0.50 mm). We find at a stagnation pressure of 50 torr and a nozzle diameter of 0.5 mm a Boltzmann distribution characterized by a vibrational temperature of  $153 \pm 5^\circ\text{K}$  and a rotational temperature of  $55 \pm 10^\circ\text{K}$ . Beams under different stagnation conditions have essentially the same internal state distribution. Studies of  $\text{K}_2$  dimers produced in a nozzle beam with various stagnation pressures (20–300 torr) and a 0.25 mm nozzle throat diameter also show cooling in both vibrational and rotational modes. A search is made for atomic fluorescence arising from the photodissociation of dimers in high vibrational levels of the ground state. No evidence is found for the presence of vibrationally-excited dimers in the nozzle beam.

## INTRODUCTION

Ever since Kantrowitz and Grey<sup>1</sup> first proposed the supersonic jet expansion of gases as a high intensity source, these so-called "nozzle beams" have offered the promise of (1) making available strongly-forward-peaked beam fluxes orders of magnitude greater than in conventional effusive flows; (2) preparing beam molecules in known and controllable nonequilibrium distributions that differ radically from the nozzle temperature; and (3) creating high concentrations of unusual beam aggregates through the condensation of supersaturated vapor. This has encouraged a number of research groups to exploit nozzle beams to carry out reactive and nonreactive scattering experiments, to study the structural properties of the nozzle beam molecules through molecular beam resonance techniques, and to investigate termolecular collision processes and nucleation kinetics.<sup>2</sup> Our own interest in nozzle beams has been stimulated by the desire to create a concentrated, collision-free source of alkali dimers so that the excited-state properties of these molecules could be investigated by level-crossing techniques.<sup>3</sup> However, in the course of these studies we have become intrigued by the dynamics of formation of these molecules.

The expansion of a gas through a nozzle leads to a highly directed mass flow in the form of a beam. The nozzle beam derives its translational energy from its own internal energy and from its random motion, so that a cooling of the gas occurs. As the gas expands, collisions become progressively less frequent. The vibrational and rotational modes, initially at equilibrium with translation, have different relaxation rates and are deactivated more slowly than the translational mode. This results first in a departure from vibrational equilibrium and then from rotational equilibrium. At lower temperatures and pressures the rates of energy transfer decrease and the vibrational and rotational distributions "freeze" corresponding to higher temperatures  $T_{\text{vib}}$  and  $T_{\text{rot}}$  than the translational temperature of the nozzle beam.

There have been many studies, both theoretical and experimental, devoted to characterizing the quantum states of the nozzle-beam molecules.<sup>2,4</sup> Information has been obtained about the internal state distribution using electron-beam-excited fluorescence,<sup>5</sup> optical line reversal,<sup>6</sup> and molecular beam electric resonance<sup>7</sup> and deflection.<sup>8</sup> All these experimental studies found cooling of the nozzle-beam molecules. However, interest in this subject has been stimulated by the recent work of Gordon, Lee, and Herschbach<sup>9</sup> (GLH), who studied the velocity distribution of  $\text{Rb}_2$  and  $\text{Cs}_2$  dimers generated in a supersonic nozzle expansion. They also measured the excess mole fraction of  $\text{Rb}_2$  and  $\text{Cs}_2$  over equilibrium using magnetic deflection analysis. Based on energy balance considerations, they suggested that roughly half (i.e.,  $6 \pm 4$  kcal/mole) of the heat of dimerization for dimers formed in the nozzle expansion downstream from the nozzle is trapped as vibrational excitation of the dimer molecules. These studies were extended to  $\text{K}_2$  by Foreman, Kendall, and Grice<sup>10</sup> (FKG), who inferred that approximately one-third (i.e.,  $4 \pm 4$  kcal/mole) of the heat of dimerization appears as vibrational excitation of the  $\text{K}_2$  dimers formed downstream.

We report here a new technique for the study of the internal state distribution of nozzle-beam molecules, namely that of white-light and laser-induced fluorescence. We have applied this technique to study  $\text{Na}_2$  and  $\text{K}_2$  dimers found in a nozzle beam. Our operating conditions for  $\text{Na}_2$  are varied from  $pd=25$  torr·mm to  $pd=120$  torr·mm corresponding to approximate stagnation Reynolds numbers<sup>11</sup> ranging from 650 to 2600. For  $\text{K}_2$ ,  $pd$  ranges from  $pd=5$  torr·mm to  $pd=75$  torr·mm corresponding to stagnation Reynolds numbers of about 155 to 2150. In all cases, we find that appreciable cooling occurs in both the rotational and vibrational structure of the dimer molecules.

## APPARATUS

The beam source is a double oven constructed from 304 stainless steel. It consists of an oven chamber

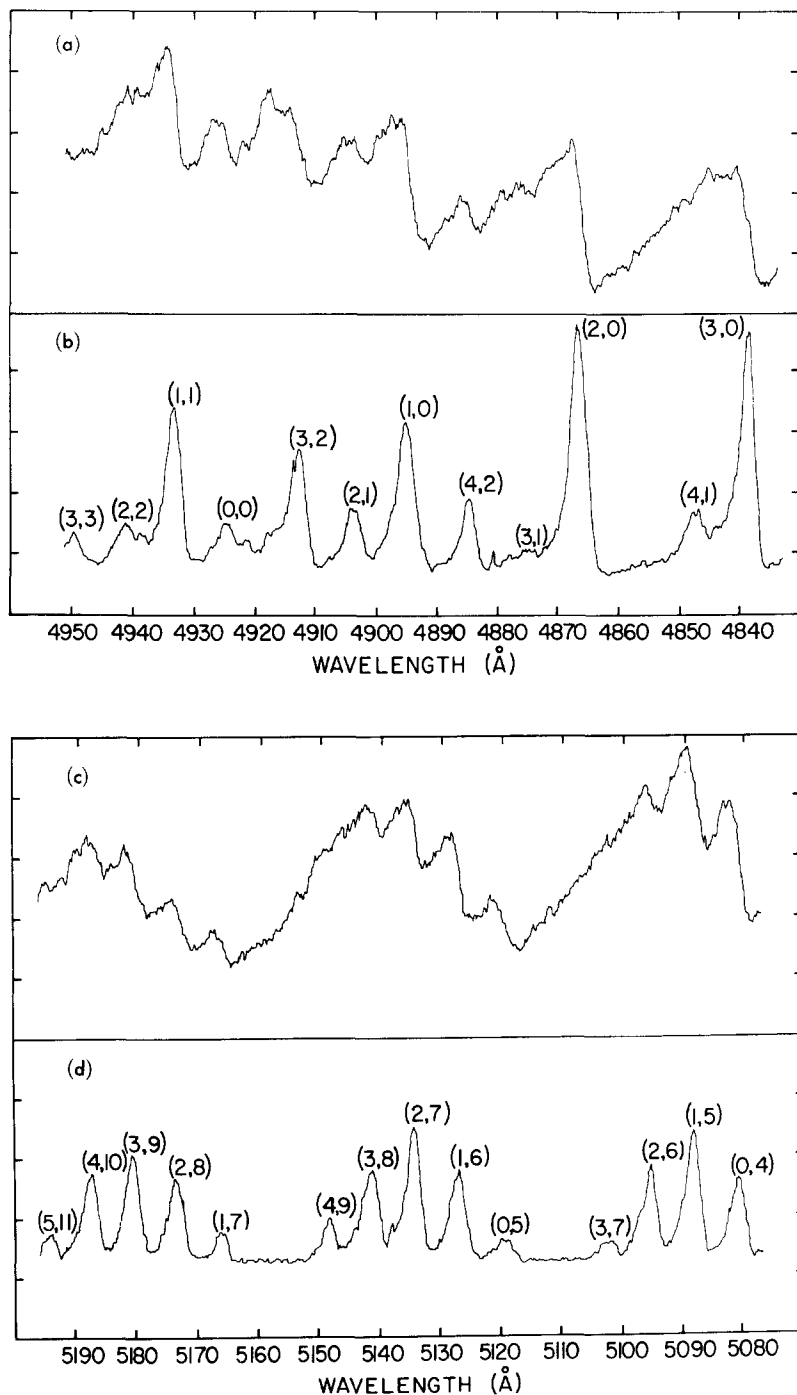


FIG. 1. The  $\text{Na}_2 B^1\Pi_u - X^1\Sigma_g^+$  fluorescence spectrum excited by white light (a) and (c) in a cell at  $590^\circ\text{K}$  and (b) and (d) in a nozzle beam with an oven chamber temperature of  $920^\circ\text{K}$ , and a nozzle chamber temperature of  $970^\circ\text{K}$ . The vibrational bands are identified by  $(v', v'')$ .

(10.2 cm long and 6.4 cm in diameter) and a nozzle chamber (2.0 cm long and 3.2 cm in diameter). Different nozzles are attached to the latter by means of a knife-edge seal on a Ta gasket. The nozzle design is similar to that of GLH<sup>9</sup> and to that of Beck and Morgenstern.<sup>12</sup> We use nozzles with throat diameters of 0.12 to 0.50 mm; the latter being about 4 times larger than a typical nozzle throat diameter used by GLH. The oven is supported on 4 tungsten pins and it is enclosed in a stainless-steel radiation shield, a

water-cooled copper shield, and a liquid-nitrogen-cooled brass shield. Holes are cut in these shields to line up with the nozzle; this provides collimation of the beam. High purity (99.95%) sodium metal and moderate purity (99%) potassium metal is used.<sup>13</sup> The oven chamber and the nozzle chamber are heated with separate windings of thermocoax heating wire INcI 15.<sup>14</sup>

For most of the  $\text{Na}_2$  runs, the oven chamber is maintained at a temperature of  $920^\circ\text{K}$ , corresponding to a pressure of 50 torr of sodium. The  $\text{K}_2$  runs are

TABLE I. List of relative populations  $N_{v'}$  and  $N_v$  of the  $\text{Na}_2$  molecules in the nozzle beam, based on the fluorescent intensities of the  $(v', v'')$  bands.

Band ( $v', v''$ )	Intensity $I(v', v'')$ (arbitrary units)	Frequency ( $\text{cm}^{-1}$ ) $\nu$	$q_{v'v''}$ <sup>a</sup>	Photomultiplier response	$N_{v'}$	Vibrational level $v$	$N_v/N_0$
(0, 2)	21.7	19 988.2	0.269	0.381	0.132	0	1
(1, 0)	24.8	20 424.8	0.161	0.415	0.213	1	$2.19 \times 10^{-1}$
(2, 0)	37.1	20 546.1	0.213	0.419	0.233	2	$5.94 \times 10^{-2}$
(3, 0)	32.6	20 666.0	0.200	0.420	0.213	3	$1.07 \times 10^{-2}$
(4, 2)	9.4	20 470.7	0.074	0.416	0.174	4	$4.98 \times 10^{-2}$

<sup>a</sup> Values are taken from Ref. 12.

carried out for oven chamber temperatures between 750–950°K, corresponding to pressures of 20–300 torr of potassium. The temperature of the nozzle chamber is always about 50° higher than that of the oven chamber in order to prevent clogging of the nozzle orifice with condensed metal. The temperatures of the oven chamber and the nozzle chamber are measured separately with Chromel–Alumel thermocouples.

To attain higher alkali vapor pressures, grooves with 5/8-in. spacings were cut for the thermocoax wire on both the oven chamber and the nozzle chamber. In addition, the heater elements were enclosed in stainless-steel covers that were tightened with screws. With these modifications that ensure better thermal contact, we were able to heat the oven chamber to 1055°K (corresponding to 240 torr of sodium pressure) and the nozzle chamber to 1100°K.

The beam flux is monitored with a hot tungsten wire (0.12 mm diameter) surface ionization detector, which may be scanned across the beam profile to provide a rough indication of the angular distribution of the beam flux. When the beam becomes supersonic the angular distribution becomes sharply peaked. The molecular beam apparatus is evacuated with a 6 in. oil diffusion pump (2400 liters/sec) having a water-cooled baffle. The oven chamber is loaded with alkali metal under a nitrogen atmosphere and then the system is evacuated over a 12 h period. During an experimental run, the background pressure is about  $1 \times 10^{-6}$  torr in the expansion chamber.

The expansion chamber consists of a 29 cm long Pyrex bell jar to which sidearms with Pyrex windows have been attached. Either white light from an Oriol Xe–Hg (1000 W) lamp or the output from a Carson cw argon ion laser (500 mW) is passed through the sidearms (windows) of the bell jar at right angles to the alkali beam. The resulting fluorescence is viewed at right angles to both the excitation light beam and the molecular beam where it is reflected by means of a mirror into either a 3/4 m SPEX 1702 spectrometer with an uncooled EMI 6256 QA photomultiplier (S-11 response) or a 1 m Interactive Technology Inc. spectrometer with a cooled Centronics Q4283 photomultiplier (extended S-20 response). The photoelectric signal

is detected with a Keithley 417 picoammeter and the fluorescence spectrum is displayed on a Leeds and Northrup strip-chart recorder.

In the case of the  $\text{Na}_2$  runs, a heated, evacuated cell containing sodium vapor is used to obtain reference measurements at a known cell temperature for which all the molecular modes are at thermal equilibrium. The cell is constructed from Corning 1720 glass and fluorescence measurements are made at right angles to the exciting light beam.

## RESULTS

### Fluorescence with White Light

A portion of the  $\text{Na}_2$   $B^1\Pi_u - X^1\Sigma_g^+$  fluorescence spectrum obtained with white-light excitation is shown in Fig. 1 for a cell at 590°K [Figs 1(a) and 1(c)] and for the supersonic nozzle beam with an oven chamber temperature of 920°K and a nozzle throat diameter of 0.5 mm [Figs. 1(b) and 1(d)]. A comparison of the cell fluorescence with the nozzle-beam fluorescence reveals that the latter is remarkably simpler in appearance with well-resolved vibrational band heads. The relative intensities of the band heads in Figs. 1(b) and 1(d) are obtained by measuring the areas under the respective bands. Table I summarizes our findings where corrections have been made for spectral response of the detection optics and for the lack of flatness of the white light source.

By determining the upper-state vibrational distribution, the ground-state distribution may be evaluated from the former in the following manner. The emission intensity of a  $v'J' \rightarrow v''J''$  line in the absence of radiative transfer complications is approximately given by

$$I(v'J'; v''J'') = KN_{v',J'} q_{v',v''}^A(v'J'; v''J'') \bar{R}_e^2 q_{v',v''} [S_{J',J''} / (2J'+1)], \quad (1)$$

where  $K$  is a proportionality constant depending on the geometry of the detection system,  $N_{v',J'}$  is the population in the  $(v', J')$  level,  $\nu(v'J'; v''J'')$  is the frequency of the transition,  $\bar{R}_e$  is the average electronic transition moment,  $q_{v',v''}$  is the Franck–Condon factor of the  $(v', v'')$  band, and  $S_{J',J''}$  is the Hönl–London

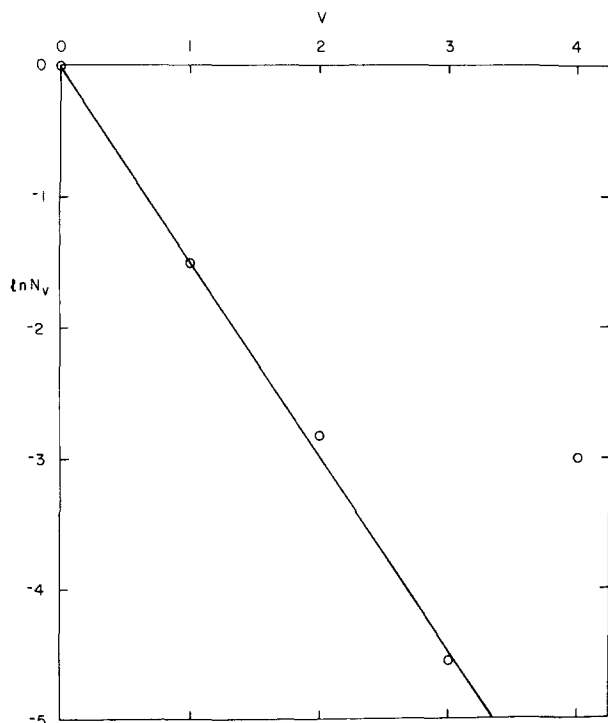


FIG. 2. Plot of  $\ln N_v$  vs  $v$ . The experimental points are shown by open circles and the least-squares fit to the first four points by a solid line.

factor. The emission intensity of a vibrational band can be obtained from Eq. (1) by summing over all  $J'$  lines of the band, i.e.,

$$I(v', v'') = KN_{v'} \nu^4 \bar{R}_v^2 q_{v', v''}, \quad (2)$$

where  $N_{v'}$  is the population of the  $v'$  level and  $\nu$  is the frequency of the  $v', 0-v'', 0$  transition. Thus the relative populations of the vibrational level  $v'$  may be found from the expression  $I(v', v'')/\nu^4 q_{v', v''}$ , i.e. from a knowledge of the emission intensity, the Franck-Condon factor, and the transition frequency of the band. With the Franck-Condon factors and spectroscopic constants given by Demtröder, McClintock, and Zare,<sup>15</sup> the relative vibrational populations  $N_{v'}$  have been calculated and the results are also given in Table I.

In the resonance fluorescence process we designate the initial ground state vibrational-rotational levels by  $(v, J)$  and the final ground state vibrational-rotational levels by  $(v'', J'')$ . For excitation by a white light source with constant intensity over the wavelength region of interest, each vibrational population factor  $N_{v'}$  will be proportional to the sum of the populations  $N_v$  of the different initial  $v$  levels weighted by their respective Franck-Condon factors and transition frequencies:

$$N_{v'} = C \sum_{v=0}^{v_{\max}} N_v q_{v', v} \nu(v', v). \quad (3)$$

The summation extends over all initial bound vibra-

tional levels. However, because the nozzle beam is quite cold, as can be seen from Fig. 1, only the lowest vibrational levels will be appreciably populated and we may truncate the summation in Eq. (3) by setting  $v_{\max}=4$ . From the measured values of  $N_{v'}$ , we may determine the values of  $N_v$  by inverting the set of equations represented by Eq. (3).

The  $N_v$  values found in this manner are given in the last column of Table I where we have normalized all values to  $N_{v=0}=1$ . Figure 2 shows a least squares plot of  $\ln N_v$  versus  $v$  for  $N_0, \dots, N_3$  from which it is seen that the vibrational distribution of the  $\text{Na}_2$  molecules in the nozzle beam corresponds to a Boltzmann distribution with a temperature  $T_{\text{vib}}=153 \pm 5^\circ\text{K}$ . Here the error represents the statistical uncertainty (one standard deviation) in our measurements. The value  $N_4$  does not lie on the straight line shown in Fig. 2. However, we are hesitant to attribute much significance to this deviation because (1) the smallest value of  $N_v$  is most sensitive to the errors in  $N_{v'}$ , and (2)  $N_4$  represents the contribution from all higher  $v$  levels. We have found that if we solve for  $N_0, N_1, N_2$ , and  $N_3$  the values of the logarithms of  $N_0, \dots, N_2$  again lie on a straight line of nearly the same slope, whereas  $\ln N_3$  deviates to a higher value.

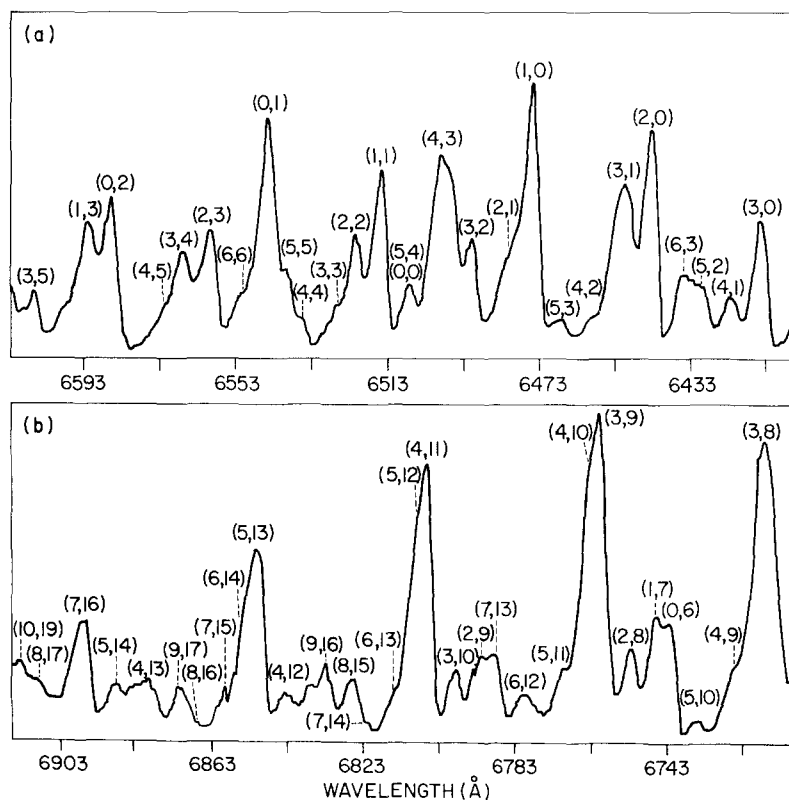
The nozzle-beam operating conditions were varied. In particular, white-light fluorescence studies were carried out at  $pd=240 \text{ torr} \times 0.5 \text{ mm} = 120 \text{ torr} \cdot \text{mm}$  corresponding to the dimer concentration of about 46% in the vibrationally frozen flow (downstream beam).<sup>9</sup> Again, a sharply defined band structure results which is essentially identical to that shown in Fig. 1. No additional bandhead features are observed.

Studies of  $\text{K}_2$  molecules in a supersonic nozzle expansion are also performed using white light excitation. As in the case of  $\text{Na}_2$ , sharply defined vibrational bandheads appear in fluorescence as shown in Fig. 3. The  $\text{K}_2$  bandheads are much narrower than those observed from a cell at about  $575^\circ\text{K}$ .<sup>15</sup> Although the cooling is pronounced, no effort was made to extract a vibrational temperature because of the overlapping  $\text{K}_2$  bands. Unlike the  $\text{Na}_2$  fluorescence spectrum (see Fig. 1), the  $\text{K}_2$  fluorescence spectrum (Fig. 3) has bands extending to high  $v''$  values. This is a consequence of the fact that at a given temperature higher  $v''$  levels of the  $\text{K}_2 X$  state are populated.

#### Fluorescence Induced by Laser Lines

The laser-induced fluorescence spectrum of  $\text{Na}_2$  has been investigated previously using the various lines of the cw argon ion laser.<sup>16</sup> In particular, as shown in Fig. 4, the 4765 Å line excites two different fluorescence series, one originating from the  $v=0, J=28 \rightarrow v'=6, J'=27$  transition, the other from the  $v=3, J=13 \rightarrow v'=10, J'=12$  transition. Figure 4(a) pertains to fluorescence from a cell; Fig. 4(b) refers to fluorescence from the nozzle beam. By comparing the relative

FIG. 3. The  $K_2 B^1\Pi_u - X^1\Sigma_g^+$  fluorescence spectrum excited by white light in a nozzle beam with an oven chamber temperature of 860°K, and a nozzle chamber temperature of 910°K. The vibrational bands are identified by  $(v', v'')$ .



intensities of the same fluorescence lines in the cell and in the nozzle beam, the rotational temperature of the nozzle beam molecules may be determined from our previous measurement of the vibrational temperature.

In the case of laser-induced fluorescence, the intensity of an emission line is given by Eq. (1). It follows that the population of the  $(v', J')$  level is propor-

tional to

$$N_{v',J'} \propto v(vJ; v'J') N_{v,J} q_{vv'} [S_{J',J} / (2J'+1)]. \quad (4)$$

For thermal equilibrium<sup>17</sup>

$$N_{v,J} = N g_{\text{rot}} g_{\text{nuo}} \exp\{-[G(v) - G(0)]/kT\} \times \exp\{-[F_v(J) - F_v(0)]/kT\} / Q_{\text{vib-rot}}(T), \quad (5)$$

FIG. 4.  $\text{Na}_2$  fluorescence spectrum excited by the 4765 Å argon ion laser line (a) in a cell at 523°K and (b) in a nozzle beam with the same conditions as in Fig. 1. The  $P$  and  $R$  fluorescent lines from the two series  $v'=10, J'=12 \rightarrow v'', J''$  and  $v'=6, J'=27 \rightarrow v'', J''$  are identified by the notation  $PR(v', v'')$ . The lines from the cell are sharper than those in the beam because the former are observed with a 50  $\mu$  slitwidth while the latter is with a 100  $\mu$  slitwidth of the spectrometer.

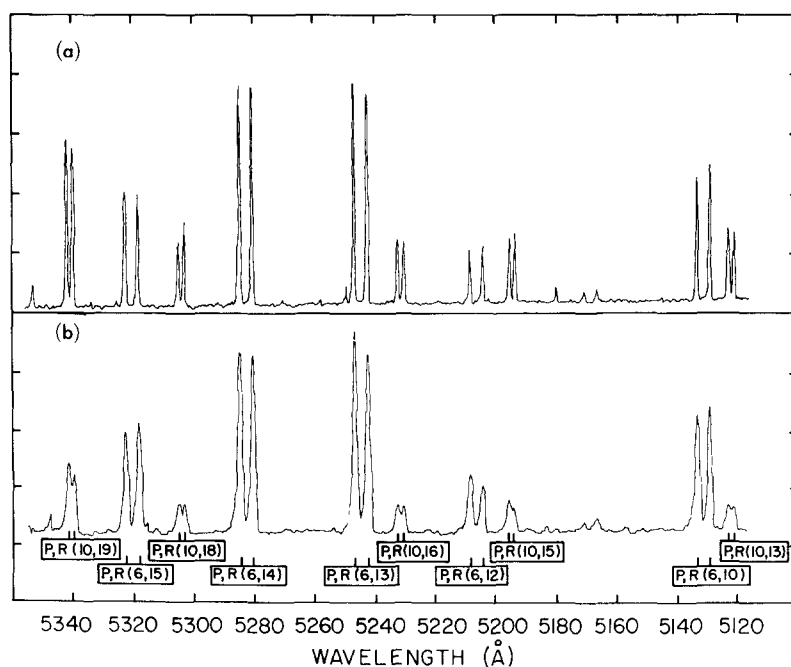


TABLE II. Rotational temperature of Na<sub>2</sub> molecules in the nozzle beam calculated from the fluorescent intensities of vibrational-rotational lines excited by the 4765 Å laser line.

Fluorescence line $v' = 10, J' = 12 \rightarrow v'', J''$	Intensity (arbitrary units)		Fluorescence line $v' = 6, J' = 27 \rightarrow v'', J''$	Intensity (arbitrary units)		$[I^{\text{cell}}/I^{\text{beam}}]_{v=3, J=13 \rightarrow v'=10, J'=12}$ $[I^{\text{cell}}/I^{\text{beam}}]_{v=0, J=28 \rightarrow v'=6, J'=27}$	$T_{\text{rot}}$ (°K)
	Cell	Beam		Cell	Beam		
$v'', J'' = 13, 11$	23.2	8.8	$v'', J'' = 10, 26$	46.2	43.4	2.5	56
15, 11	23.8	8.2	12, 26	20.0	16.2	2.2	53
16, 11	21.5	8.8	13, 26	71.5	62.0	2.1	53
18, 11	29.1	10.2	14, 26	73.8	62.0	2.4	55
19, 11	54.5	20.5	15, 26	38.5	38.5	2.6	57
20, 11	41.0	13.8	16, 26	12.5	11.6	2.7	58

where  $T$  is the temperature,  $k$  is the Boltzmann constant,  $0.695 \text{ cm}^{-1}/^\circ\text{K}$ ,  $Q_{\text{vib-rot}}$  is the vibration-rotation partition function, and the  $g$ 's are the appropriate statistical weights. Let the temperature of the cell be denoted by  $T$  and let  $T_{\text{vib}}$  and  $T_{\text{rot}}$  be the vibrational

and rotational temperatures, respectively, of the molecules in the beam. Then the ratio of the fluorescence intensity of a line in the cell to that of the same line in the beam can be expressed with the help of Eqs. (1), (4), and (5) as

$$[I^{\text{cell}}/I^{\text{beam}}]_{vJ \rightarrow v'J'} = K' \frac{\exp\{-[G(v) - G(0)]/kT\}}{\exp\{-[G(v) - G(0)]/kT_{\text{vib}}\}} \frac{\exp\{-[F_v(J) - F_v(0)]/kT\}/Q_{\text{vib-rot}}(T)}{\exp\{-[F_v(J) - F_v(0)]/kT_{\text{rot}}\}/Q_{\text{vib-rot}}(T_{\text{vib}}, T_{\text{rot}})}, \quad (6)$$

where  $K'$  is a constant of proportionality that depends on (1) geometrical factors in viewing the fluorescence from the cell and from the beam, and (2) the extent of optical pumping<sup>18</sup> in the cell and in the beam.

Let us form the ratio of  $I^{\text{cell}}/I^{\text{beam}}$  for the two different fluorescence series. As long as the viewing geometry and the extent of optical pumping (laser-induced bleaching) is the same for the two fluorescence series,<sup>19</sup> we may write

$$\frac{[I^{\text{cell}}/I^{\text{beam}}]_{v=3, J=13 \rightarrow v'=10, J'=12}}{[I^{\text{cell}}/I^{\text{beam}}]_{v=0, J=28 \rightarrow v'=6, J'=27}} = \frac{\exp\{-[G(3) - G(0)]/kT\} \exp\{-[F_3(13) - F_0(28)]/kT\}}{\exp\{-[G(3) - G(0)]/kT_{\text{vib}}\} \exp\{-[F_3(13) - F_0(28)]/kT_{\text{rot}}\}} \quad (7)$$

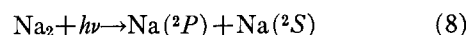
and  $T_{\text{rot}}$  may be determined from a knowledge of  $T$ ,  $T_{\text{vib}}$ , and  $I^{\text{cell}}/I^{\text{beam}}$  for the two series. The calculations are summarized in Table II. We find that  $T_{\text{rot}} = 55 \pm 10^\circ\text{K}$  where the uncertainty of this result depends linearly on the errors in the vibrational temperature of the beam and in the temperature of the cell. Our error in  $T_{\text{rot}}$  also includes the statistical scatter shown in Table II.

In addition, we attempted to excite fluorescence in the K<sub>2</sub> nozzle beam using the He-Ne laser. The beam conditions were the same as for the white-light fluorescence study of K<sub>2</sub> described in the previous section. The 6328 Å He-Ne laser line excites a number of resonance fluorescence series in K<sub>2</sub> in a cell.<sup>20</sup> The strongest fluorescence progressions arise from the following transitions:  $(v=0, J=82) \rightarrow (v'=7, J'=81)$  and  $(v=1, J=72) \rightarrow (v'=8, J'=72)$  in the  $B^1\Pi_u - X^1\Sigma_g^+$  red band system. We were unable to detect fluorescence in the nozzle beam. Because these transitions involve high  $J$  values, the absence of fluorescence offers further evidence for the rotational cooling of the K<sub>2</sub> dimers found in the lowest vibrational levels in the nozzle beam.

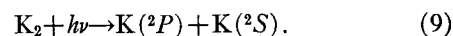
#### Search for Photofragment Fluorescence

According to the Franck-Condon principle, molecules in high vibrational levels of the ground state of Na<sub>2</sub> or K<sub>2</sub> preferentially make transitions to the continuum levels rather than to the bound vibrational

levels of the  $B^1\Pi_u$  state.<sup>21</sup> Such a transition dissociates the Na<sub>2</sub> or K<sub>2</sub> molecules into one excited and one unexcited alkali atom:



and



The excited alkali atom may be detected by its characteristic emission.

A search was made for the sodium  $D$  lines in both white-light-induced and laser-induced fluorescence. This was carried out for various operating conditions of the nozzle beam. In the case of white-light excitation, Corning filters and interference filters are used to block light in the incident beam that can excite atomic sodium fluorescence. All wavelengths longer than or shorter than the cutoff value of about 5890 Å were excluded in different runs. In the latter case there is no atomic emission observed, while in the former case, we are able to detect a faint Na  $D$  line signal with 500 μ slits. However, the signal is found to be independent of operating conditions. It possibly originates from the near-resonant excitation transfer process,  $\text{Na}_2^* + \text{Na} \rightarrow \text{Na}^* + \text{Na}_2$ , although direct photodissociation from Na<sub>2</sub> molecules in  $v'' \geq 6$ , for example, cannot be ruled out.

A similar search was made for the potassium  $D_1$  and  $D_2$  lines at 7699 and 7665 Å, respectively, using white-light-induced fluorescence. Again care was taken to

remove radiation that can excite directly the potassium atoms in the beam. This is accomplished by inserting different Corning filters in the incident light path. In particular, we used Corning filter 1-56, 4-67, 4-97, and 7-56 in different runs. We find a K atom fluorescence signal for the first three filters that transmit light primarily in the region of 3900–7000 Å, which can excite the cold K<sub>2</sub> molecules. For the Corning 7-56 filter, which transmits light with wavelengths greater than 7700 Å, no atomic fluorescence is observed. We also used cutoff interference filters manufactured by Optics Technology, Inc., one with a cutoff at wavelengths greater than 6500 Å, another at 6000 Å. In both cases, we observe atomic fluorescence as well as molecular band fluorescence.

We have also studied the atomic fluorescence signal as a function of wavelength of the incident light by placing several Corning filters: 0-51, 7-59, 3-75, 3-73, 3-72, 3-70, 3-68, successively in front of other filters located in the path of the incident light beam. Use of a filter that blocks wavelengths shorter than 4100 Å removes the atomic signal completely. Thus the atomic fluorescence requires photons of wavelengths less than 4100 Å. The lower limit of wavelengths of the incident light in our experiment is controlled by the focussing Pyrex lens and the Pyrex window. With the thickness of the lens and the window there is less than 10% transmission below 3900 Å. This shows that the origin of the potassium *D* lines is caused by the direct excitation of potassium atoms to the 5<sup>2</sup>*P* state, corresponding to excitation at 4047 Å. The branching ratios<sup>22</sup> for the 5<sup>2</sup>*P*→4<sup>2</sup>*S* transition is 0.25. The remaining fraction (0.75) of the excited (5<sup>2</sup>*P*) atoms cascade down to the ground state through the intermediate 4<sup>2</sup>*P* state emitting the characteristic potassium *D*<sub>1</sub> and *D*<sub>2</sub> lines.

By examining the Franck-Condon factors for the K<sub>2</sub> B<sup>1</sup>Π<sub>u</sub>–X<sup>1</sup>Σ<sub>g</sub><sup>+</sup> system, we find that molecules with  $v'' \gtrsim 15$  will contribute significantly to photofragment fluorescence, e.g., for

$$v'' = 15, \quad \sum_{v'=0}^{15} q_{v',15} = 0.48.$$

It seems reasonable to assume that molecules in high vibrational levels will absorb white light about equally as well as molecules in low vibrational levels. If 1% of the total fluorescence signal were concentrated in the potassium *D*<sub>1</sub> and *D*<sub>2</sub> lines, it would be detected in our experimental setup. Hence, the absence of atomic fluorescence when the nozzle beam is irradiated by light of 4100–7000 Å indicates that the fraction of vibrationally excited molecules ( $v'' \gtrsim 15$ ) in the beam must be quite small (less than a few percent).

## DISCUSSION

The formation dynamics of nozzle beam dimers are conveniently described using the dimensionless reduced variables introduced by GLH,<sup>9</sup> namely the reduced temperature  $\bar{T}$ , the reduced density  $\bar{\rho}$ , and the reduced nozzle throat diameter  $\bar{w}$ . Using the principle of corre-

sponding states Hagen<sup>23</sup> has shown that nozzle expansions of "similar" gases with the same reduced parameters will produce the same dimer yields. In particular, by using a soft-sphere model for vibrationally frozen flow, GLH have calculated the dimer mole fraction as a function of the reduced variables, and their results are presented in graphical form in Fig. 12 of their paper. For sodium our nozzle beam operating conditions range from  $\bar{w}=10$  to 40,  $\bar{T}=0.1$ , and  $\bar{\rho}=1.4 \times 10^{-5}$  to  $7 \times 10^{-5}$ . From Fig. 12 of GLH we find that the total dimer concentration of Na<sub>2</sub> in our experiment is predicted to vary from 15% to 45% of which 2% to 17% are formed downstream from the nozzle during expansion. For potassium our nozzle beam operating conditions of  $p=200$  torr stagnation pressure, and  $d=0.025$  cm throat diameter correspond to the reduced variables  $\bar{w}=12$ ,  $\bar{T}=0.16$ , and  $\bar{\rho}=1.35 \times 10^{-4}$ . Here Fig. 12 of GLH (see their curve marked  $\bar{T}=0.2$  and  $\bar{w}=10$ ) shows that of the 18% K<sub>2</sub> dimer concentration in the vibrationally frozen flow, about 3% is present initially in equilibrium with the atoms in the nozzle chamber while the remaining 15% are formed downstream from the nozzle in the hydrodynamic flow.<sup>24</sup> Thus, while in the case of sodium a small fraction of the dimers are expected to be formed downstream, in the case of potassium almost all the dimers are formed downstream. It is to be noted that it is these "downstream dimers" that are believed to be vibrationally "hot" because of insufficient collisional relaxation.

Indirect evidence for the existence of hot alkali dimer molecules in nozzle beam expansions has been obtained by GLH and by FKG based on measurements of the translational energy of the dimer molecules. We would expect the presence of hot alkali dimers to manifest itself in our optical studies through (1) the appearance of new bandhead features and (2) in an enhanced atomic fluorescence signal arising from photodissociation of the hot dimers. Moreover, we would expect that (1) and (2) would vary with the concentration of downstream dimers, and hence vary with operating conditions. Our observations for both sodium and potassium nozzle beams do not support the existence of any significant fraction of such vibrationally excited dimers.

Indeed, under our working conditions, we conclude that the dimer molecules in the nozzle beam have been appreciably cooled. Because the dimer molecules are thus concentrated in the lowest rotational and vibrational levels of the molecule, such dimer beams simplify the studies of their optical, microwave, ESR, and molecular beam resonance spectra. In the case of optical studies, this may allow one to achieve in the gas phase the benefits of matrix isolation spectroscopy without the disadvantages of matrix interactions.

## ACKNOWLEDGMENTS

We thank Professor J. B. Fenn and Professor D. R. Herschbach for many useful conversations on this topic.

- \*Support by the National Science Foundation is gratefully acknowledged.
- <sup>†</sup>Present address: Fakultät für Physik der Universität, Freiburg, Germany.
- <sup>1</sup>A. Kantrowitz and J. Grey, *Rev. Sci. Instrum.* **22**, 328 (1951).
- <sup>2</sup>J. B. Anderson, R. P. Andres, and J. B. Fenn, *Adv. Chem. Phys.* **10**, 275 (1966).
- <sup>3</sup>R. N. Zare, *Acc. Chem. Res.* **4**, 361 (1971).
- <sup>4</sup>For a review of vibrational relaxation see J. W. Rich and C. E. Treanor, *Annu. Rev. Fluid Mech.* **2**, 355 (1970). For a discussion of rotational relaxation see V. O. Hagena and W. Henkes, *Z. Naturforsch. A* **15**, 851 (1960); E. L. Knuth, *Appl. Mech. Rev.* **17**, 751 (1964); H. Ashkenas, *Phys. Fluids* **10**, 2509 (1967); D. R. Miller and R. P. Andres, *J. Chem. Phys.* **46**, 3418 (1967); B. Lefkowitz and E. L. Knuth in *Adv. Appl. Mech.*, Suppl. 5 Vol. II, 1421 (1969) and references cited therein; J. J. Repetski and R. E. Mates, *Phys. Fluids* **14**, 2605 (1971).
- <sup>5</sup>E. P. Muntz, *Phys. Fluids* **5**, 80 (1962); P. V. Marrone, *Phys. Fluids* **10**, 521 (1967); F. Robben and L. Talbot, *Phys. Fluids* **9**, 644 (1966).
- <sup>6</sup>T. A. Holbeche and J. G. Woodley, *AGARD Conf. Proc.* **2**, 507 (1967).
- <sup>7</sup>T. R. Dyke, G. R. Tomasovitch, W. Klemperer, and W. E. Falconer, "Electric Resonance Spectroscopy of Hypersonic Molecular Beams," *J. Chem. Phys.* **57**, 2277 (1972).
- <sup>8</sup>P. J. Dagdigian (private communication); P. J. Dagdigian, J. Graff, and L. Wharton, *J. Chem. Phys.* **55**, 4980 (1971).
- <sup>9</sup>R. J. Gordon, Y. T. Lee, and D. R. Herschbach, *J. Chem. Phys.* **54**, 2393 (1971).
- <sup>10</sup>P. B. Foreman, G. M. Kendall, and R. Grice, *Mol. Phys.* **23**, 117 (1972).
- <sup>11</sup>Estimated using the viscosity data of D. I. Lee, Ph. D. thesis, Columbia University, New York, 1967.
- <sup>12</sup>D. Beck and R. Morgenstern, Diplomarbeit, Physikalisches Institut der Universität, Freiburg, Germany, 1967.
- <sup>13</sup>The Na and K metals are obtained from A. D. MacKay, New York, New York. For runs at the highest oven temperatures a 99% pure Na metal sample is used. High purity K metal was also used for a few runs.
- <sup>14</sup>Thermocoax wire (Amperex Electronics Corporation, Hicksville, New York) consists of a central Ni-Cr alloy wire insulated from the external sheath of Inconel with a highly compressed packing of MgO, thus obviating the need of electrical insulation of the heating element from the metal oven.
- <sup>15</sup>We thank Jeannine Toueg for providing us with her K<sub>2</sub> fluorescence traces taken by irradiating a cell of potassium vapor with white light.
- <sup>16</sup>W. Demtröder, M. McClintock, and R. N. Zare, *J. Chem. Phys.* **51**, 5495 (1969).
- <sup>17</sup>G. Herzberg, *Spectra of Diatomic Molecules* (D. Van Nostrand-Reinhold Co., New York, 1950).
- <sup>18</sup>R. E. Drullinger and R. N. Zare, *J. Chem. Phys.* **51**, 5532 (1969).
- <sup>19</sup>We have found that at higher laser powers (>130 mW), the lines of the two series are pumped at a constant ratio both in the cell and the beam. In Eq. (7) we have dropped the term  $\exp\{-[F_0(0) - F_3(0)]/kT\}/\exp\{-[F_0(0) - F_3(0)]/kT_{rot}\}$  which is very close to unity (1.00004).
- <sup>20</sup>W. J. Tango, J. K. Link, and R. N. Zare, *J. Chem. Phys.* **49**, 4264 (1968).
- <sup>21</sup>For the higher vibrational levels  $v''$  of the ground state the summation of Franck-Condon factors over all *bound* vibrational levels  $v'$  of the upper state is less than unity, i.e.,  $\sum_{v'} q_{v''v'} < 1$ . The deviation from unity of this sum indicates that fraction that can make transitions to the upper-state continuum.
- <sup>22</sup>O. S. Heavens, *J. Opt. Soc. Am.* **51**, 1058 (1961).
- <sup>23</sup>O. F. Hagena, *Advan. Appl. Mech.*, Suppl. 5 **2**, 1465 (1969).
- <sup>24</sup>GLH in their explanatory footnotes 54 and 71 state that Fig. 12 may be an overestimate because of various reasons. However, the results of FKG show that this may not be the case for potassium. In their experimental run with oven body temperature of  $\approx 870^\circ\text{K}$  (corresponding to potassium vapor pressure of  $\approx 120$  torr) and nozzle temperature of  $\approx 900^\circ\text{K}$  and a nozzle throat diameter of 0.008 cm, FKG find that the dimer constitutes about 25% in the vibrationally frozen flow compared with  $\approx 3\%$  in the oven vapor. The corresponding value of dimer molecules in the beam from Fig. 12 of GLH is less than 8% in the vibrationally frozen flow.